

Mode-locked Tm,Ho:KLu(WO₄)₂ laser at 2060 nm using InGaSb-based SESAMs

Veselin Aleksandrov,^{1,2} Alexander Gluth,¹ Valentin Petrov,¹ Ivan Buchvarov,²
Günter Steinmeyer,^{1,3} Jonna Paajaste,³ Soile Suomalainen,³ Antti Härkönen,³
Mircea Guina,³ Xavier Mateos,⁴ Francesc Díaz,⁴ and Uwe Griebner^{1,*}

¹Max Born Institute for Nonlinear Optics and Short Pulse Spectroscopy, Max-Born-Str. 2A, 12489 Berlin, Germany

²Physics Department, Sofia University, 5 James Bourchier Blvd., 1164 Sofia, Bulgaria

³Optoelectronics Research Centre, Tampere University of Technology, P.O. Box 692, 33101 Tampere, Finland

⁴Física i Cristal·lografia de Materials i Nanomaterials, Universitat Rovira i Virgili, Campus Sescelades, c/ Marcel·li Domingo, s/n, 43007-Tarragona, Spain

*griebner@mbi-berlin.de

Abstract: Passive mode-locking of a Tm,Ho:KLu(WO₄)₂ laser operating at 2060 nm using different designs of InGaAsSb quantum-well based semiconductor saturable absorber mirrors (SESAMs) is demonstrated. The self-starting mode-locked laser delivers pulse durations between 4 and 8 ps at a repetition rate of 93 MHz with maximum average output power of 155 mW. Mode-locking performance of a Tm,Ho:KLu(WO₄)₂ laser is compared for usage of a SESAM to a single-walled carbon nanotube saturable absorber.

©2015 Optical Society of America

OCIS codes: (140.4050) Mode-locked lasers; (140.5680) Rare earth and transition metal solid-state lasers.

References and links

1. F. Dausinger, F. Lichtner, and H. Lubatschowski, *Femtosecond Technology for Technical and Medical Applications* (Springer, 2004).
2. P. A. Budni, L. A. Pomeranz, M. L. Lemons, C. A. Miller, J. R. Mosto, and E. P. Chicklis, "Efficient midinfrared laser using 1.9- μ m pumped Ho:YAG and ZnGeP₂ optical parametric oscillators," *J. Opt. Soc. Am. B* **17**(5), 723–728 (2000).
3. M. Ebrahim-Zadeh and I. T. Sorokina, *Mid-infrared Coherent Sources and Applications* (Springer, 2008).
4. N. Coluccelli, G. Galzerano, D. Gatti, A. Di Lieto, M. Tonelli, and P. Laporta, "Passive mode-locking of a diode-pumped Tm:GdLiF₄ laser," *Appl. Phys. B* **101**(1-2), 75–78 (2010).
5. A. A. Lagatsky, S. Calvez, J. A. Gupta, V. E. Kisel, N. V. Kuleshov, C. T. A. Brown, M. D. Dawson, and W. Sibbett, "Broadly tunable femtosecond mode-locking in a Tm:KYW laser near 2 μ m," *Opt. Express* **19**(10), 9995–10000 (2011).
6. A. Gluth, X. Mateos, J. Paajaste, S. Suomalainen, A. Härkönen, M. Guina, G. Steinmeyer, S. Veronesi, M. Tonelli, J. Li, Y. Pan, J. Guo, V. Petrov, and U. Griebner, "Passively mode-locked Tm:YAG ceramic laser at 2 μ m," in *Advanced Solid State Lasers*, (Optical Society of America, 2013), paper AF1A.2.
7. A. A. Lagatsky, F. Fusari, S. Calvez, S. V. Kurilchik, V. E. Kisel, N. V. Kuleshov, M. D. Dawson, C. T. A. Brown, and W. Sibbett, "Femtosecond pulse operation of a Tm,Ho-codoped crystalline laser near 2 μ m," *Opt. Lett.* **35**(2), 172–174 (2010).
8. A. A. Lagatsky, X. Han, M. D. Serrano, C. Cascales, C. Zaldo, S. Calvez, M. D. Dawson, J. A. Gupta, C. T. A. Brown, and W. Sibbett, "Femtosecond (191 fs) NaY(WO₄)₂ Tm,Ho-codoped laser at 2060 nm," *Opt. Lett.* **35**(18), 3027–3029 (2010).
9. K. J. Yang, D. C. Heinecke, C. Kölbl, T. Dekorsy, S. Z. Zhao, L. H. Zheng, J. Xu, and G. J. Zhao, "Mode-locked Tm,Ho:YAP laser around 2.1 μ m," *Opt. Express* **21**(2), 1574–1580 (2013).
10. K. Yang, D. Heinecke, J. Paajaste, C. Kölbl, T. Dekorsy, S. Suomalainen, and M. Guina, "Mode-locking of 2 μ m Tm,Ho:YAG laser with GaInAs and GaSb-based SESAMs," *Opt. Express* **21**(4), 4311–4318 (2013).
11. N. Coluccelli, A. Lagatsky, A. Di Lieto, M. Tonelli, G. Galzerano, W. Sibbett, and P. Laporta, "Passive mode locking of an in-band-pumped Ho:YLiF₄ laser at 2.06 μ m," *Opt. Lett.* **36**(16), 3209–3211 (2011).
12. W. B. Cho, A. Schmidt, J. H. Yim, S. Y. Choi, S. Lee, F. Rotermund, U. Griebner, G. Steinmeyer, V. Petrov, X. Mateos, M. C. Pujol, J. J. Carvajal, M. Aguiló, and F. Díaz, "Passive mode-locking of a Tm-doped bulk laser near 2 μ m using a carbon nanotube saturable absorber," *Opt. Express* **17**(13), 11007–11012 (2009).
13. J. Liu, Y. Wang, Z. Qu, and X. Fan, "2 μ m passive Q-switched mode-locked Tm³⁺:YAP laser with single-walled carbon nanotube absorber," *Opt. Laser Technol.* **44**(4), 960–962 (2012).

14. A. Schmidt, S. Y. Choi, D. Yeom, F. Rotermund, X. Mateos, M. Segura, F. Díaz, V. Petrov, and U. Griebner, "Femtosecond pulses near 2 μm from a Tm:KLuW laser mode-locked by a single-walled carbon nanotube saturable absorber," *Appl. Phys. Express* **5**(9), 092704 (2012).
15. J. Ma, G. Xie, P. Lv, W. Gao, P. Yuan, L. Qian, U. Griebner, V. Petrov, H. Yu, H. Zhang, and J. Wang, "Wavelength-versatile graphene-gold film saturable absorber mirror for ultra-broadband mode-locking of bulk lasers," *Sci. Rep.* **4**, 5016 (2014).
16. A. A. Lagatsky, Z. Sun, T. S. Kulmala, R. S. Sundaram, S. Milana, F. Torrisi, O. L. Antipov, Y. Lee, J. H. Ahn, C. T. A. Brown, W. Sibbett, and A. C. Ferrari, "2 μm solid-state laser mode-locked by single-layer graphene," *Appl. Phys. Lett.* **102**(1), 013113 (2013).
17. V. Aleksandrov, A. Gluth, V. Petrov, I. Buchvarov, S. Y. Choi, M. H. Kim, F. Rotermund, X. Mateos, F. Díaz, and U. Griebner, "Tm,Ho:KLu(WO₄)₂ laser mode-locked near 2 μm by single-walled carbon nanotubes," *Opt. Express* **22**(22), 26872–26877 (2014).
18. U. Keller, "Recent developments in compact ultrafast lasers," *Nature* **424**(6950), 831–838 (2003).
19. S. Anikeev, D. Donetsky, G. Belenky, S. Luryi, C. A. Wang, J. M. Borrego, and G. Nichols, "Measurement of the Auger recombination rate in p-type 0.54 eV GaInAsSb by time-resolved photoluminescence," *Appl. Phys. Lett.* **83**(16), 3317–3319 (2003).
20. G. Benz and R. Conradt, "Auger recombination in GaAs and GaSb," *Phys. Rev. B* **16**(2), 843–855 (1977).
21. J. Paajaste, S. Suomalainen, R. Koskinen, A. Härkönen, G. Steinmeyer, and M. Guina, "GaSb-based semiconductor saturable absorber mirrors for mode-locking 2 μm semiconductor disk lasers," *Phys. Stat. Solidi C* **9**(2), 294–297 (2012).
22. J. Paajaste, S. Suomalainen, A. Härkönen, U. Griebner, G. Steinmeyer, and M. Guina, "Absorption recovery dynamics in 2 μm GaSb-based SESAMs," *J. Phys. D* **47**(6), 065102 (2014).
23. V. Jambunathan, A. Schmidt, X. Mateos, M. C. Pujol, U. Griebner, V. Petrov, C. Zaldo, M. Aguiló, and F. Díaz, "Crystal growth, optical spectroscopy and continuous-wave laser operation of co-doped (Ho,Tm):KLu(WO₄)₂ crystals," *J. Opt. Soc. Am. B* **31**(7), 1415–1421 (2014).
24. M. Moenster, U. Griebner, W. Richter, and G. Steinmeyer, "Resonant saturable absorber mirrors for dispersion control in ultrafast lasers," *IEEE J. Quantum Electron.* **43**(2), 174–181 (2007).

1. Introduction

The development of ultrashort pulse Tm- and Ho-based bulk lasers emitting in the 2 μm spectral range is presently a subject of intensive study. It is motivated by potential applications, especially in laser surgery [1] and for the generation of coherent mid-infrared radiation using optical parametric conversion [2,3]. Since 2009 passive mode-locking of bulk lasers operating around 2 μm has been obtained using two types of saturable absorbers: semiconductor saturable absorber mirrors (SESAMs) and carbon-nanostructure-based saturable absorbers (single-walled carbon nanotubes or graphene). SESAMs have been successfully used for the full variety of Tm-, Tm,Ho- and Ho-based bulk lasers [4–11] whereas carbon-nanostructure-based saturable absorbers have been restricted to Tm- and Tm,Ho-lasers [12–17]. However, despite the recent progress of saturable absorber technology around 2 μm , saturable absorbers have not reached the maturity level of those utilized in the spectral range around 1 μm yet. The main challenge for realization of ultrashort pulse bulk lasers around 2 μm is still the improvement of the saturable absorber properties, in particular, their absorption recovery time, non-saturable losses, and damage threshold.

Compared to SESAMs [18], saturable absorbers based on single-walled carbon nanotubes (SWCNT) and graphene possess intrinsically fast recovery times on the order of 1 ps as well as low saturation fluences and modulation depths [12,15]. However, their power handling capability in mode-locked oscillators appears limited by the required embedding of the SWCNTs in a resin, typically in PMMA. The fragile single layer structure of graphene on a substrate imposes similar limitations. In contrast, GaAs- and InP-based SESAMs are fabricated by mature technologies and exhibit very low scattering losses, but their absorption recovery time amounts to tens or hundreds of picoseconds. In turn, the long recovery time of the absorber degrades the mode-locking performance of the laser. To the end of accelerating the recovery process, advanced growth and post-growth processing techniques, such as low-temperature growth, ion irradiation/implantation, or the use of surface quantum wells (QWs), have been developed. Nevertheless, using these methods, it seems inevitable to accelerate the recovery without also increasing non-saturable losses of SESAMs.

Compared to other SESAMs, GaSb-based ones (GaInAsSb/AlGaAsSb QWs) possess relatively low non-saturable losses, and their recovery time is orders of magnitude shorter than that of GaAs- and InP-based devices [19,20]. The ultrafast absorption recovery time in

such high quality hetero-structures is attributed to significantly stronger Auger recombination than in GaAs and InP hetero-structures, and it is independent of growth temperature and strain in the QWs [21,22]. In recent years, irradiation with As^+ ions was employed for further speeding up the recovery of the GaSb-based SESAMs. The latter SESAMs were successfully implemented in 2 μm mode-locked bulk lasers [5,7,8,11]. As a result of our recent studies, near-surface placement of the QWs and additional anti-reflection (AR) coating appear to offer a unique alternative opportunity for tailoring the recovery time of GaSb-based SESAMs [22].

Here we report passive mode-locking of a $\text{Tm,Ho:KLu(WO}_4)_2$ (Tm,Ho:KLuW) laser employing InGaSb-based SESAMs designed as few QW or near-surface QW structures. They are AR-coated and optimized for fast carrier relaxation without the introduction of additional losses, which leads to reliable pulse performance of the laser. The SESAM mode-locked Tm,Ho:KLuW laser results are compared to those obtained with SWCNTs as saturable absorber in a similar laser configuration [17].

2. Experimental set-up

The laser set-up is based on a standard X-shaped cavity with length of 1.6 m (Fig. 1). The active medium (AM) is a 3 mm long Tm,Ho:KLuW crystal, grown by the Top Seeded Solution Growth technique with 5 at.% Tm^{3+} - and 0.5 at.% Ho^{3+} -doping in the solution [23]. In this class of monoclinic biaxial crystals, the gain bandwidths are very broad, and the absorption and emission cross-sections are exceptionally high for selected polarizations. The active medium is mounted in a water cooled copper holder. The crystal is positioned under Brewster angle. Beam orientation is chosen for propagation along the N_g crystallographic axis and for polarization along the N_m axis. The pump source is a continuous-wave Ti:sapphire laser, generating more than 2 W of output power at 802 nm. The pump beam is focused into the active medium at a radius of $\sim 30 \mu\text{m}$. The single pass absorption of the Tm,Ho:KLuW crystal in the lasing state is 87% and about 95% for double-pass pumping.

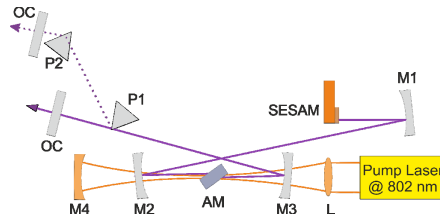


Fig. 1. Layout of the Tm,Ho:KLuW laser. AM: active medium; L: focusing lens; M1: concave mirror (radius of curvature $\text{RoC} = 50 \text{ mm}$); M2, M3 and M4: concave mirrors ($\text{RoC} = 100 \text{ mm}$); M1, M2, M3: highly reflective at 2060 nm and highly transmitting at 800 nm; M4: highly reflective at 800 nm; P1 and P2: CaF_2 -prisms; OC: output coupler.

Two curved folding mirrors (M2 and M3) ensure TEM_{00} operation with 30- μm cavity waist radius where the active medium is positioned. One of the cavity arms contains an additional focusing mirror (M1) to increase the intensity on the SESAM which acts as an end mirror. The cavity waist radius at the position of the SESAM is $\sim 30 \mu\text{m}$. The other arm contains the plane output coupler. In the latter arm, two CaF_2 -prisms can optionally be inserted.

The employed SESAMs are based on GaSb hetero-structures with some modifications. They were grown on a (100) n-GaSb substrate by molecular beam epitaxy. First, a GaSb-buffer was grown followed by a lattice-matched AlAsSb/GaSb distributed Bragg reflector consisting of 18.5 pairs. The absorber region is anti-resonant at the operating wavelength of 2 μm and consists of 10-nm thick InGaAsSb QWs embedded in GaSb. The samples contain three, two, or one QW. Furthermore they exhibit a different thickness of the GaSb cap layer. All samples are AR-coated by means of a dielectric $\text{TiO}_2/\text{SiO}_2$ double layer. The parameters of the SESAMs are listed in Table 1. The absorption recovery dynamics of the SESAMs were characterized in a noncollinear cross-polarized pump-probe measurement setup. For this purpose, a commercial optical parametric oscillator (Spectra Physics) was used delivering

180-fs pulses at 2040 nm. The resulting pump pulse fluence on the sample amounted to $\sim 50 \mu\text{J}/\text{cm}^2$. As revealed by the pump-probe measurements, all SESAMs show a very similar intraband (fast component) relaxation time $\tau_1 < 0.5$ ps. The interband relaxation time τ_2 (slow component) for the SESAMs with the QWs placed 10 nm below the surface is $\tau_2 < 5$ ps and appears slightly decreased compared to those with at least 10 times thicker cap layers. This reduction is explained by fast recombination via surface states. In SESAM No.2, employing two QWs, the reduction of τ_2 due to surface recombination is not as strong as in SESAMs No.3 and No.4 since the second QW is already twice the cap layer thickness away from the surface. We therefore conclude that the variation of τ_2 is systematic and explained by surface effects. The samples incorporating one QW and a cap layer thickness < 10 nm (No.3 and 4) exhibit lowest values of τ_2 .

3. Experimental results

Passive mode-locking is obtained with all the four SESAMs, using output coupler transmissions (T_{OC}) of 1.5%, 3% and 5%. Table 1 lists the achieved pulse parameters of the mode-locked Tm;Ho:KLuW laser for all SESAMs.

Best performance in terms of stability and output power is achieved with SESAM No.2. Using SESAM No.1 the shortest pulse duration of $\tau_p = 4.2$ ps is obtained. This is attributed to its 3-QW structure, corresponding to the highest available modulation depth. For the 1-QW near-surface structures (No.3 and No.4) exhibiting the lowest modulation depth, the pulse durations are roughly twice the duration of No.1, and a weak tendency toward multi-pulse operation is observed.

Table 1. Parameters of the SESAMs under investigation and obtained experimental results with mode-locking of Tm,Ho:KLuW laser ($T_{OC} = 3\%$, τ_2 : SESAM relaxation time, τ_p : mode-locked pulse duration).

SESAM	Number of QWs	GaSb-cap thickness (nm)	τ_2 (ps)	τ_p (ps)	P_{out} (mW)
No.1	3	300	9.7	4.2	110
No.2	2	5	4.1	7.0	150
No.3	1	10	1.7	7.2	140
No.4	1	5	1.6	7.8	150

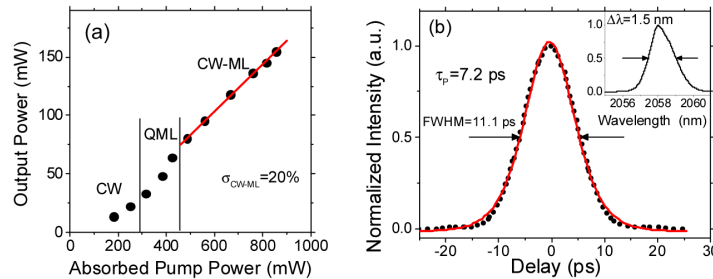


Fig. 2. SESAM mode-locked Tm,Ho:KLuW laser ($T_{oc} = 3\%$, SESAM No.2): (a) output vs. input characteristics (dots) and linear fit in the mode-locked (CW-ML) regime (red line); (b) autocorrelation curve (black dots), fit assuming sech^2 pulse shape (red line) and optical spectrum (inset).

The output vs. pump power characteristics of the Tm,Ho:KLuW laser using SESAM No.2 and $T_{OC} = 3\%$ are shown in Fig. 2. The laser starts running in continuous-wave (CW) operation at a threshold pump power of 150 mW. The threshold for mode-locked operation (CW-ML) corresponds to an absorbed pump power of 450 mW, Fig. 2(a). Below this threshold, mode-locking is disturbed by some Q-switching instabilities (QML). The mode-locked laser operates at a repetition rate of 93 MHz, and the maximum output power amounts to 155 mW at an absorbed pump power of 860 mW, resulting in a slope efficiency $\sigma_{CW-ML} = 20\%$. At an absorbed pump power higher than 900 mW, multi-pulse operation is observed. To characterize the pulse duration, we used a commercial autocorrelator (APE *pulseCheck* SM, extended IR). The measurement principle is based on second harmonic generation at $2 \mu\text{m}$ to

retrieve the autocorrelation trace. The derived pulse duration at maximum output power is 7.2 ps, under assumption of a sech^2 -pulse shape, see Fig. 2(b). The measured optical spectrum is centered at 2058 nm with a FWHM of 1.5 nm, inset Fig. 2(b). The calculated time-bandwidth product $\tau_p \Delta\nu = 0.76$, corresponds to ≈ 2 times the Fourier limit and indicates slightly chirped pulses. However, no significant pulse shortening is observed when the two CaF_2 -prisms are introduced into the cavity for dispersion management.

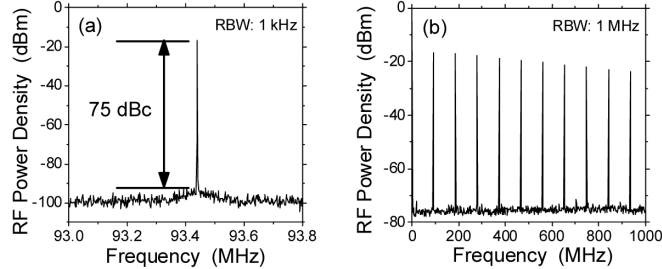


Fig. 3. Radio frequency spectra of the SESAM mode-locked Tm,Ho:KLuW laser ($T_{oc} = 3\%$, SESAM No.2): (a) fundamental beat note, (b) 1 GHz wide-span; RBW: resolution bandwidth.

The measured radio-frequency spectra of the SESAM mode-locked laser show the fundamental beat note at 93.4 MHz, Fig. 3(a), measured with a resolution bandwidth of 1 kHz, and the 1 GHz wide-span measurement, Fig. 3(b). The high extinction ratio of 75 dBc and the absence of spurious modulation indicate stable mode-locking operation.

4. Discussion

We employed a similar laser configuration for mode-locking the Tm,Ho:KLuW laser at 2060 nm, now using SWCNTs as saturable absorber [17]. At nearly the same repetition rate the achieved pulse duration (slightly shorter: $\tau_p = 2.8$ ps) and the average output power (slightly lower: $P_{out} = 97$ mW) were comparable to the SESAM mode-locked laser. The main difference is related to the time-bandwidth product $\tau_p \Delta\nu$. Emitting the same spectral bandwidth of ~ 1.5 nm (FWHM), the SWCNT-SA mode-locked laser generates almost transform-limited pulses ($\tau_p \Delta\nu = 0.32$) whereas the resulting value $\tau_p \Delta\nu$ is 0.76 with use of the SESAM. The latter value is a clear indication that clean soliton mode-locking could not be obtained here, and that pulse generation completely relies on the action of the SESAM here. In such a situation, one expects to obtain a pulse duration near the slow relaxation time constant of the SESAM. In fact, all pulse durations and absorber time constants lie in the range from 1 to 10 ps. Nevertheless, there is also a clear anti-correlation between pulse duration and absorber time constant in the data compiled in Table 1. Considering that the fastest SESAMs 3 and 4 exhibit equally fast relaxation as the previously employed SWCNT [17], we conclude that there must exist an additional limiting mechanism. Inspecting the group delay dispersion (GDD), the overall round-trip cavity GDD was negative for both lasers with the main contribution from the gain medium, $GDD \sim -1040$ fs². The transmission-type SWCNT-SA in [17] was deposited on a silica substrate, contributing a GDD of ~ -115 fs². The total GDD of ~ -1155 fs² therefore appears to support nearly ideal transform-limited pulses, whereas the SESAM structure seem to have less favorable dispersion values. To verify this hypothesis, we computed the GDD of the layer structures. As a basis for these computations, we used the measured and designed reflectivity of SESAM No.3 shown in Fig. 4, revealing differences between the original design and the measurement. First, one can see that the Bragg reflector appears narrower and slightly shifted relative to the design. This difference is indicative of a deviation of the refractive index data in the actually grown structure relative to design data. Moreover, these uncertainties in the semiconductor index data also appear to have degraded the antireflection performance, the design of which relies on exact knowledge of index data. Figure 4 also shows the designed GDD of the SESAM structure. Here we deduce ~ -700 fs² for the SESAM GDD, resulting in an overall GDD of \sim

1740 fs², which is larger compared to the cavity containing the SWCNT-SA. Gires-Tournois effects [24] may further contribute to this value.

In any case, for operating the laser in the soliton-like regime, the net negative GDD seems to be too high. This may be one reason for the inferior pulse quality with SESAM. A second problem may arise from the relatively large third-order dispersion (TOD) of the slightly decentered Bragg reflector. Neither of these potential problems can be reduced by insertion of the prism sequence into the cavity. The prism compressor can only deliver negative GDD and TOD of the same sign as the Bragg stack near 2 μm wavelength, which probably explains the unsuccessful experiments in this direction.

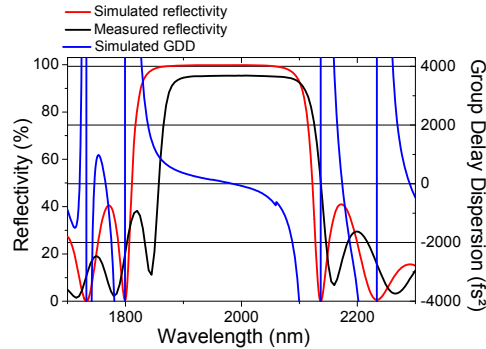


Fig. 4. InGaSb-based SESAM (No.3); measured and calculated reflectivity and calculated group delay dispersion. The reflectivity measurement has an error margin of 2%. Dispersion calculation is based on assumption of a near-ideal two-layer dielectric coating that is perfectly matched to the index of the top layer semiconductor.

Additionally, our experiments indicate the important role of the modulation depth. We observe pulse shortening with increased modulation depth for the employed GaSb-based SESAM, Table 1. One strategy to generate shorter pulses in the femtosecond range using Tm,Ho:KLuW could therefore be employing a higher modulation depth of GaSb-based SESAMs with suitable correction of the dispersion, either by adapted design of AR coating and Bragg stack or by insertion of corrective GTI mirrors. Unfortunately, measured data of the SESAM modulation depths are not available yet. However, the evaluated insertion loss at the lasing wavelength of 2060 nm ranged between 3% and 6% depending on the number of QWs in the samples. This estimation takes into account the error margin of the reflectivity measurement of 2% and the deduced peak absorption of ~1.5% per QW.

For the case of SWCNT-SA mode-locking of the Tm,Ho:KLuW laser, it seems to us that further optimization may barely be possible as the modulation depth is difficult to increase, which would inevitably require thicker SWCNT layers with higher scattering loss.

5. Conclusion

SESAM mode-locking of a Tm,Ho:KLuW laser is reported for the first time to our knowledge. Different designs of GaSb-based QW SESAMs including near-surface structures are compared with respect to their mode-locking performance. The obtained mode-locking stability and the pulse duration between 4 ps and 8 ps can be ascribed to specific SESAM design parameters, in particular the modulation depth. Compared to the previously reported performance of mode-locked Tm,Ho-codoped lasers, the presented results appear quite encouraging. Applying such SESAMs designed with slightly higher modulation depth and an improved dispersion management, we expect further pulse shortening into the sub-ps range with the Tm,Ho:KLuW laser, which is intended as a next step.

Acknowledgments

We acknowledge support from the bilateral exchange programme between Germany and Bulgaria (DAAD Project-ID 54391860).